DOI: 10.14258/jcprm.20260418421

UDC 582.52:581.4; 574.24

BIRCH LIGNINS: CHEMICAL DIVERSITY AND THORIUM-232 SORPTION PROPERTIES*

© ***A.P. Karmanov[1]**, L.S. Kocheva[2], N.G. Rachkova[1], O.Yu. Derkacheva[3]***

[1] Institute of Biology of the Komi Science Center UB RAS, st. Kommunisticheskaya, 28, Syktyvkar, 167982, Russia, apk0948@yandex.ru
[2] Institute of Geology of the Komi Science Center UB RAS, st. Pervomaiskaya, 54, Syktyvkar, 167982, Russia
[3] Saint Petersburg State University of Industrial Technologies and Design, st. Bolshaya Morskaya, 18, Saint Petersburg, 191186, Russia

This article presents the results of a comprehensive study on the chemical structure, spectral, paramagnetic, and adsorption properties of lignins extracted from different vegetative organs of *Betula verrucosa* birch. Investigations of the sorption-desorption dynamics of the radioactive isotope Th-232 in various aqueous media revealed that lignin derived from the tree trunk exhibits the highest adsorption efficiency. This sample demonstrated exceptional retention capacity for Th-232 in water, saline solutions, and hydrochloric acid, achieving irreversible sorption of up to 95.4% of the radionuclide. Our analysis of surface-porous properties indicated that high specific surface area did not necessarily correlate with superior sorption performance. Structural characterization revealed distinct macromolecular topologies: trunk lignin adopts a star-shaped polymer configuration, whereas lignins from branches, roots, and a growth on the trunk exhibit randomly branched architectures. These results do not contradict our hypothesis that the polymer topology can influence the sorption capacity of lignin. Further analysis suggests that chemisorption, mediated by ionogenic functional groups, plays a pivotal role in the strong and selective adsorption of Th-232. The results contribute to the growing database on lignin biomedical potential, paving the way for the development of novel, high-performance enterosorbents.

Keywords: adsorption; lignins; thorium-232; topology structure.

For citing: Karmanov A.P., Kocheva L.S., Rachkova N.G., Derkacheva O.Yu. *Khimiya Rastitel'nogo Syr'ya*, 2026, no. 4, Online First. (in Russ.). https://doi.org/10.14258/jcprm.20260418421.

Introduction

As is known, the Earth crust contains rocks with small but significant concentrations of various natural radionuclides (RN), including thorium-232. Mineral raw materials used in technological processing may also contain various long-lived radionuclides in concentrations significantly exceeding background levels. Nuclear power facilities create a significant radiation load on the environment and the population [1]. Water is the main medium that determines the transfer of thorium in the environment. Usually, the concentrations of this element in surface waters are quite low. The concentration of thorium-232 in natural aquatic environments fluctuates in the range of 10^{-7}–1 μg/ml [2]. The permissible concentration of thorium-232 should not exceed 0.05 μg/ml. The highest values are observed in regions with increased thorium content in parent rocks, as well as in areas of uranium, tin and rare earth element mining. The results of modern studies show that even small doses of ionizing radiation have an adverse effect on human biological systems [3, 4]. In particular, thorium causes disturbances in the spleen, liver, hematopoietic organs, nervous system, which in the long term can result in oncological diseases.

Anthropogenic processes, including the sedimentation, dissolution and migration of thorium and other RN, consistently cause pollution of both underground and surface water resources. Radioactive elements, entering the ecosystem through water migration processes, are integrated into food chains, initiating a sequential biogeochemical cycle "soil-plant-animal-human". This process, known as bioaccumulation, plays a critical role in the progressive

* This article has electronic supplementary material (appendix), which is available to readers on the journal's website. DOI: 10.14258/jcprm.20260418421s

** Corresponding author.

accumulation of radionuclides within mammalian organisms, including humans [5].To ensure complete human safety, it is necessary to introduce new effective technological processes for water decontamination at municipal water treatment plants. In some cases, modern methods of efferent therapy may also offer a viable treatment pathway. Efferent therapy is based on preventive measures aimed at neutralizing and removing micro-quantities of toxins from the body using oral enterosorbents [6, 7]. With regard to radionuclides, the most effective are sorption technologies designed to decontaminate aqueous media directly in the gastrointestinal tract (GIT) of humans and animals. Among the most important properties that RN enterosorbents should have is their ability to firmly bind radioactive elements in aqueous media of various compositions with a relatively low concentration of radionuclides [8].

Expensive synthetic adsorbents with record-high sorption characteristics are not suitable in this case. It should be borne in mind that such preparations can simultaneously absorb normal microflora, which is involved in metabolic processes. In addition, enterosorbents must be quickly eliminated from the body without causing side effects and be resistant to the effects of digestive enzymes of the gastrointestinal tract. Widespread plant biopolymers – lignins meet all these requirements. According to the literature [9, 10], natural lignins do have the ability to adsorb heavy toxic metals in the form of ions from aqueous systems. However, the creation of lignin adsorbent production does not have a simple solution, since lignins, unlike cellulose, have a different chemical structure. The feasibility of searching for and developing new lignin-type enterosorbents is that lignin-based preparations are high-molecular compounds with all the characteristic and useful properties of polymers. Therefore, from the point of view of creating new-generation enterosorbents, the macromolecular nature of lignins is an undeniable advantage. This is attributed to the additional biomedical potential of natural lignin-based enterosorbents, which may exhibit immunostimulatory, oncoprotective, and geroprotective properties mediated through hepatoenteric circulation in the gastrointestinal tract [11–13]. A unique feature of natural lignins as high-molecular compounds is the polyvariability of their chemical structure depending on the botanical species of the plant [14, 15], as well as on the localization (location) of lignin in certain vegetative organs of plants. Thus, it is necessary to conduct systematic detailed studies of lignins of various origins according to the scheme: structure - properties - sorption capacity.

This article studies chemical, spectral, paramagnetic and adsorption properties of lignins from different vegetative parts (organs) of the birch *Betula verrucosa*, a widespread woody plant. Considerable attention is paid to the determination of polymer characteristics that allow establishing the topological structure of macromolecules, which is important for assessing the behavior of lignin in liquid media. One of the main tasks was to assess prospects for creating effective high-molecular sorbents designed for detoxification and removal of the long-lived radionuclide thorium-232 from water systems. This will allow expanding data on the biomedical potential of lignins for the subsequent creation of innovative biologically active enterosorbents of a new generation.

Material and Methods

Plant material and its characteristics. To obtain lignin samples, we selected a mature 35-year-old woody plant *Betula verrucosa* growing in a site with a normal level of radioactive background of 0.14±0.005 (Radiation background, μSv/h) in the Syktyvdinsky district (Komi Republic, Russia). Lignins were extracted from the trunk (sample LB-1), roots (sample LB-2), branches 3–4 cm thick (sample LB-3) and a growth on the trunk (suvel) (sample LB-4). Sample LB-1n was isolated from the trunks of the dwarf birch *Betula nana*, harvested in the tundra in the north of the Komi Republic. According to the method proposed by Pepper [16], the plant material was mechanically ground to sawdust using an ERS-750 BOXBOT reciprocating saw (China). This was followed by the process of extraction with distilled water at a temperature of 40 °C, and then extraction with a mixture of ethanol and benzene (2 : 1). According to the protocol proposed by Pepper, lignin samples were extracted using an aqueous solution of dioxane (in a ratio of 9 : 1 by volume) while boiling in the presence of hydrochloric acid (0.7% by weight). The extraction process was carried out in a nitrogen atmosphere and lasted for one hour.

Elemental analysis of the lignin samples was carried out by EA 1110 CHNS-O Analyzer (CE Instruments, Italy). The functional group content (COOH, [OH]ph and Σ(OH)a) was determined by the standard methods of lignin chemistry [17].

Fourier-transform infrared spectroscopy. The samples were subjected to Fourier transform infrared spectroscopy (FTIR) using a Shimadzu IRPrestige-21 spectrophotometer (Japan). The spectrophotometer was equipped with a DLATGS detector and was set to operate in the range of 400 to 4000 cm^{-1} with a resolution of 4 cm^{-1}. Prior to the analysis, the lignin samples were thoroughly mixed and ground with potassium bromide. The IR spectra were normalized for integral absorption in the range of 1840–770 cm^{-1}.

Electron paramagnetic resonance spectroscopy. EPR spectra were obtained by X-band (9.4 GHz) spectrometer RadioPAN SE/X-2547 (CCU "Geoscience", IG FRC Komi Science Center, Ural Branch of the Russian Academy of Sciences) at room temperature. The lignin sample weight was about 20 mg. The spectra were recorded as the first derivative of the absorption signal at an RF modulation frequency of 100 kHz. The g-factor was calibrated by LiF: Li^0 reference sample (g = 2.002288). A certified DPPH sample (g = 2.0036) with a spin count of $1.96 \cdot 10^{17}$ spins was used to estimate the concentration of paramagnetic centers. The error in determining g-factors was ±0.0003, line widths – ±0.01 mT, and N concentration – 15%, respectively. Spectra fitting was performed by Origin 5.0 software.

Pyrolysis – gas chromatography – mass spectrometry (Py-GC/MS). Pyrolysis of lignin samples was performed using a GCMS-QP2010 Plus gas chromatography-mass spectrometer with an EGA/PY-3030D pyrolyzer (Frontier lab, Japan) with smooth heating from 100 to 600 °C at a rate of 50 °C/min. The resulting products were subsequently separated using a HP-5MS column (Agilent, USA). Helium was utilized as the carrier gas. Detection products was carried out in scanning mode within the mass-to-charge ratio (m/z) range of 15 to 400. The relative abundance of S, G, and H- structures was quantified by calculating the ratios of the sums of the peak areas of chromatographically resolved monomeric phenols of these types. Identification of the pyrolysis products was achieved using the NIST 2011 and Wiley MS electronic databases.

Surface porous structure. The specific surface area and the parameters of porous structure of lignin samples were determined using the automated adsorption measurement system ASAP 2020 MP (Micromeritics, USA). The samples of lignins were studied by the method of low-temperature nitrogen adsorption (77 K). The volume Vads of the adsorbed gas was reduced to normal conditions. Instrumental measurement error was ~0.20%

Hydrodynamic studies. Lignin samples were fractionated by fractional sedimentation in the dioxane (solvent) – benzene (precipitant) system. The fractions were isolated by lyophilic drying. The velocity sedimentation coefficient s_0, translational diffusion coefficient D_0, and intrinsic viscosity [η] were measured for each fraction. We used MOM-3180 ultracentrifuge to determine S at a speed of 48×10^3 rpm. The concentration of the solution in $0.2 \times 10^{-2} < c < 0.3 \times 10^{-2}$ g/cm^3. Viscometric measurements were carried out at 25 °C in Ostwald viscometers in the range of relative viscosity values $1.1 < \eta_{rel.} < 2.5$ at DMF solvent flow time of 52.0 s. Diffusion coefficients D_0 were determined by an ultracentrifuge using the "maximum ordinate-area" method at a rotor speed of 6×10^3 rpm. The Flory-Mandelkern (FM) hydrodynamic invariant was calculated by the equation $\Phi^{1/3} P^{-1} = \eta_0 [\eta]^{1/3} s_0 N_A M_{SD}^{-2/3} (1 - \nu\rho_0)^{-1}$. The Tsvetkov-Klenin hydrodynamic invariant A_0 was calculated using the equation $A_0 = ([D] M_{SD} [\eta])^{1/.3}$. $M_{SD} = s_0 RT / D_0 (1 - \nu\rho_0)$, where $(1 - \nu\rho_0)$ – the buoyancy factor. The buoyancy factor was determined by the pycnometric method. The fractal dimension was calculated by two methods: by the value of the viscosimetric scaling index using the formula $d_f = 3/(1 + b_\eta)$ (in the numerator) and by the Kozlov-Temiraev-Sozaev equation (in the denominator): $d_f = 3 \ln M_W / [\ln M_W + \ln(7.14 k_H - 1) - \ln K_\eta - \ln k_H]$, where k_H – the Huggins constant, K_η – the proportionality coefficient in the Mark-Kuhn-Houwink-Sakurada equation (MKHS): $P_i = K_{ij} M_{sD}^{bij}$, where P_i is one of the hydrodynamic characteristics [η], D_0, s_0; $b_{ij} \equiv b_\eta$, b_D, and b_S – scaling indexes, K_{ij} – corresponding coefficients.

Results and discussion

*Assessment of the sorption properties of lignin samples in relation to thorium-232.*We have studied the processes of sorption-desorption of one of the most common heavy radionuclides in water bodies – thorium-232. As can be seen in Table 1, the highest adsorption capacity for thorium is possessed by the lignin sample LB-1, isolated from the trunk of a birch stand.

Table 1. Quantitative characteristics of the processes of adsorption-desorption of thorium-238 from an aqueous solution of thorium nitrate $Th(NO_3)_4$

Sample	A, %	D_{H2O}	$D_{CH3COONH4}$	D_{HCl}	A_F
LB-1	81.2	0	1.1	3.5	95.4
LB-2	77.4	14.5	12.2	10.2	63.2
LB-3	58.6	19.4	7.2	6.3	67.1
LB-4	78.9	20.2	8.0	38.2	33.6

The value of primary adsorption A reaches 81.2% for this sample. The lowest adsorption capacity is characteristic of LB-3 preparation, for which the value of A is equal to 58.6%, and only two-thirds of this amount (67.1%) of thorium are sorbed irreversibly. For LB-4 sample, a significant portion of the radionuclide (66.4%) is bound to the adsorbent rather weakly and can be desorbed when treated with water and aqueous solutions of CH_3COONH_4 and HCl. In contrast, for LB-1 sample, the desorption indices D are minimal, so it ultimately turned out to be the most effective among the studied lignin preparations with an chemical adsorption index A_F reaching 95.4%.

Practice shows [18], that the value of the sorption indices of adsorbents for various purposes often depends on their surface-porous characteristics, such as the specific surface area (SSA) and pore volume. The analysis of low-temperature nitrogen adsorption isotherms helps to understand adsorption properties of materials. Figure 1 shows the nitrogen adsorption isotherms for the studied lignin samples.

According to the modern classification [19], the presented isotherms are classified as type IV (a). Isotherms of this type, which are S-shaped, are usually associated with the mechanism of polymolecular adsorption. The features of the type IV isotherm include the presence of a hysteresis loop caused by capillary condensation processes in mesopores, as well as the presence of an adsorption maximum in the region of high P/P_0 values. Isotherms of a similar shape are typical of adsorbents with a small surface area and a wide distribution of pore sizes. In this case, the hysteresis loops should be classified as type H1, as indicated by such features as their strong steepness and high P/P_0 values (~0.99). Experiments with nitrogen adsorption allowed quantitatively evaluating a number of important surface-porous indicators of the samples under study (Table 2).

As follows from the obtained data, sample LB-4, isolated from the lignin sample, has the highest surface area. Accordingly, this sample has the highest value of the micropore volume V_{mic} and the total volume of all pores V_Σ. However, it is not the most effective adsorbent for thorium. The strong adsorption index A_F of this sample is 2–3 times lower than for the other samples. And on the contrary, the sample with the most modest indicators of the surface-porous structure is characterized by the highest value of the strong adsorption index A_F. This turned out to be sample LB-1, isolated from the trunk part of the birch stand.

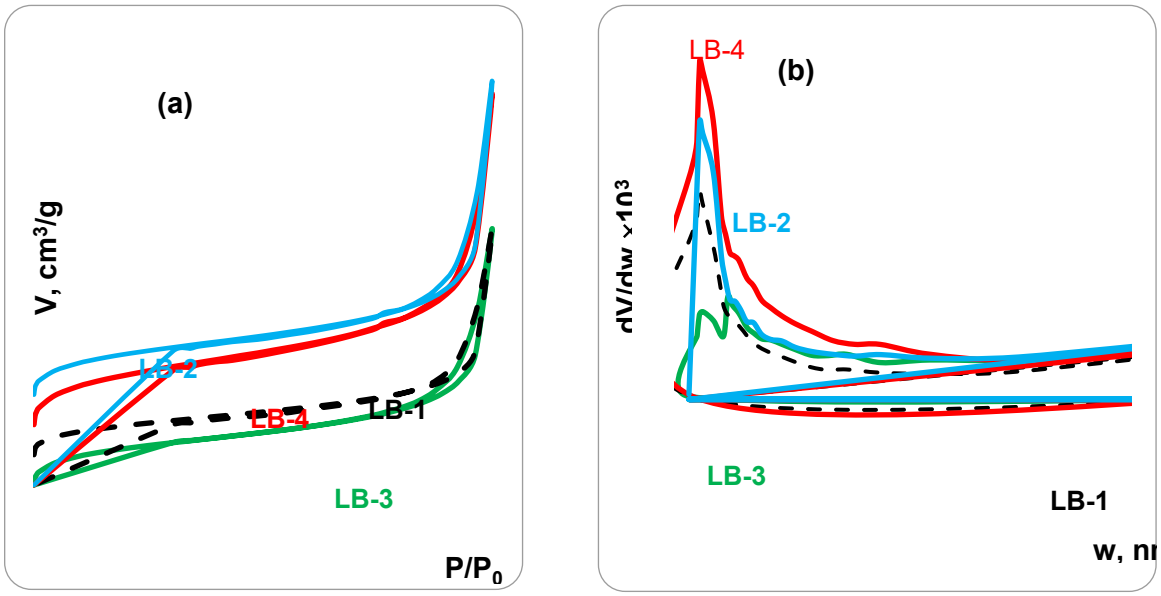


Fig. 1. Nitrogen adsorbtion isotherms (a); pore size distribution (b)

Table 2. Characteristics of surface properties of the lignin samples

Sample	SSA, m^2/g (BET)	V_Σ, $\times 10^2$ cm^3/g (BET)	V_{Ms}, $\times 10^2$, cm^3/g (BJHдес, Broekhoff-de Boer)	$V_{mic} \times 10^2$, cm^3/g (Dubinin-Radushk)	Average pore size, nm (BET)
LB-1	7.4	2.32	2.13	0.26	12.6
LB-2	10.3	3.23	1.70	0.30	12.5
LB-3	9.1	2.64	1.45	0.29	11.5
LB-4	12.7	3.41	1.79	0.39	10.8

Thus, there is no positive relationship between the surface-porous characteristics and the efficiency of thorium sorption, as evidenced by the value of the linear correlation coefficient R for the pair of SSA-A indicators, equal to 0.12. It is also of interest that the larger the surface area of the sample, the more intensive the desorption processes are when processing samples with aqueous systems. Therefore, the correlation coefficient R between S_F and SSA tends to – 1 (R=-0.98). Thus, in this case, the correlation between the surface-porous and sorption characteristics exists, however, it is negative. The next stage of the work is devoted to the consideration of the issue of the influence of the chemical factor on the processes of Th-232 sorption on natural lignins.

Characterization of Lignin Samples. Table 3 presents experimental data on the elemental composition and functional groups of the lignins. As can be seen from the obtained data, no significant differences in the elemental composition of the samples are observed. The carbon content fluctuates within 60% ± 1.1, which is consistent with previously published data [20].

At the same time, noticeable differences can be noted in the quantitative content of ionogenic functional groups: phenolic hydroxyls and carboxyl groups. The highest total amount of acidic hydroxyls (ΣOH_{sa}) was recorded in the sample isolated from the trunk of birch wood (LB-1).

FTIR Spectroscopy. FTIR spectroscopy provides important information on the structural and chemical features of lignin biopolymers [21]. In particular, the possibility of assessing the amount of key structural units of the S-, G-, H-type in lignin macromolecules is of considerable interest, since their ratio affects the functional composition and, accordingly, the reactivity and biomedical potential of lignin-based drugs. The diffuse reflectance IR spectra and the second derivatives of the spectra are shown in Figure 2 (a, b, c). The spectra of the samples LB-2, LB-3 and LB-4 are shifted vertically on the Y-axis relative to the spectrum of LD-1 on 0.4, 0.8 and 1.2 (Fig. 2a). The second derivative of spectra of the samples LB-2, LB-3 and LB-4 are shifted vertically on the Y-axis on 0.0005, 0.001 and 0.0015 in Figure 2b. Shifts of the second derivative of spectra of the samples LB-2, LB-3 and LB-4 on the Y-axis were 0.002, 0.004 and 0.006 in Figure 2c.

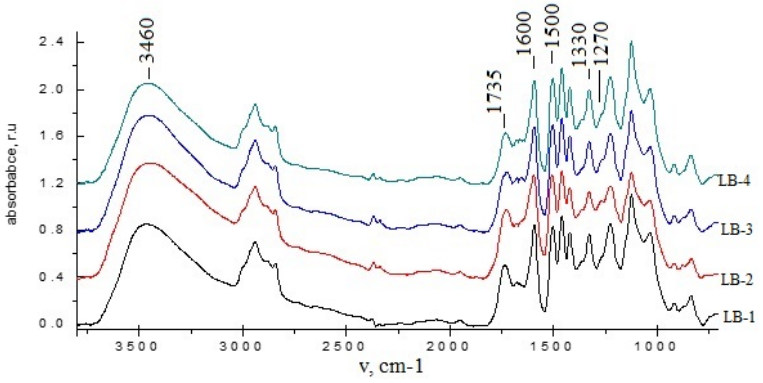
The obtained data indicate the identity of the set of absorption bands for all IR spectra, which indicates the structural similarity of the studied samples. However, certain variations in the intensity of some bands should be noted. In particular, a higher intensity of the band at 3460 cm^{-1} (stretching vibrations of OH groups) can be noted for samples LB-2 and LB-3. At the same time, the differences in the IR spectra in the absorption region of 3100–2800 cm^{-1} (νCH) are barely noticeable. Of particular interest are the differences in the intensity of the absorption bands at 1330 and 1270 cm^{-1}. As is known, the intensity of the band at 1330 cm^{-1} in the spectra of lignins indicates the amount of syringyl (S) aromatic structures, and the band at 1270 cm^{-1} is a diagnostic marker of the guaiacyl (G) type aromatic ring. Certain differences are observed for the bands with a maximum of about 1735 cm^{-1}, and for LB-2 and LB-3 samples a slight shift of the band is revealed as a result of the presence of a lower-frequency component at ~1720 cm^{-1}. This region of the spectrum is associated with vibrations of non-conjugated C=O groups. According to the nature of the second derivative of the spectra, differences are also found in the region of the bands at 1600 and 1500 cm^{-1}. The shifts of these bands in one direction or another are due to differences in the studied lignins in the number of aromatic structures of the guaiacyl and syringyl types. Particular attention was paid to identifying these differences. To calculate the number of S- and G-structures, a baseline was formed, and the spectral data were normalized to the area under the spectral curve in the range from 770 to 1840 cm^{-1}. Previously constructed calibration dependences were used for the calculations [22]. Table 4 presents the results of the calculations.

As follows from the obtained data, the studied samples belong to SG-type lignins, however, the ratio of the specified structures varies depending on the localization of lignin in various vegetative organs of the forest stand. Actually, this is quite expected, given the diversity of biological functions of lignin, on the one hand, and the different functional role of vegetative organs of plants, on the other hand. However, at present, the establishing cause-and-effect relationships is difficult. One can only note a positive relationship between the S/G indicator and strong adsorption of thorium A_F ($R \approx 0.7$). The relationship between the sorption capacity and the number of ionogenic functional groups seems more predictable. As the analysis shows, the correlation coefficient R for $OH_{ph.}$-A pair is +0.69, and for OH_{ph}-A_F pair, the coefficient is R = +0.75. If we take into account the sum of acidic hydroxyl groups ΣOH_{sa}, the correlation coefficient increases to 0.77. Although the number of samples in our experiments is small, such a comparative analysis is nevertheless valid, which is confirmed by the results of earlier works [23, 24].

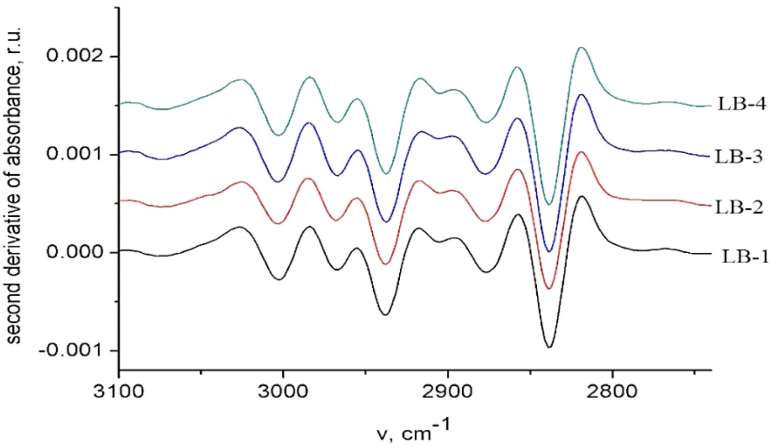
Table 3. Chemical characteristics of lignin samples, %

Sample	Hydrogen	Carbon	Nitrogen	Oxygen*	OH_{ph}	COOH	ΣOH_{sa}	OCH_3
LB-1	5.9±0.6	59.8±1.1	0.07±0.01	34.2	3.1	2.1	3.8	19.3
LB-2	6.3±0.6	59.5±0.5	0.12±0.03	34.1	2.4	2.7	3.4	17.9
LB-3	6.3±0.2	60.1±0.4	0.11±0.02	33.5	1.9	1.9	2.6	18.9
LB-4	6.2±0.3	60.4±0.6	0.08±0.03	33.3	2.1	1.5	2.6	17.5

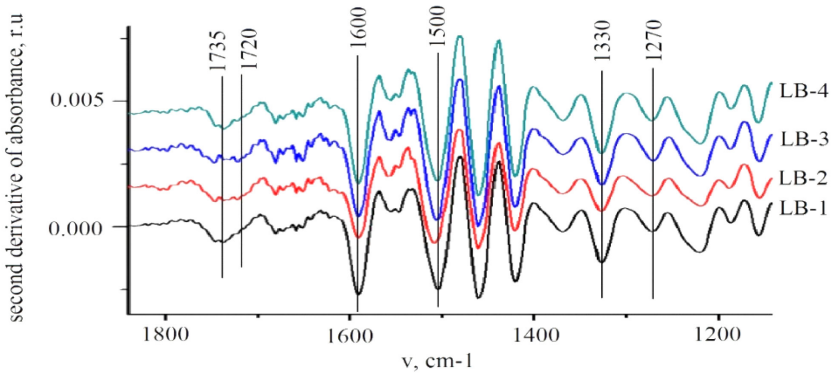
* The amount of oxygen is calculated by the difference, taking into account the amount of other elements



a



b



c

Fig. 2. IR spectra (*a*) and second derivatives of the spectra (*b* and *c*)

Table 4. The content (%) of monomeric units in lignins according to IR spectroscopy data

Sample	S	G	H*	S/G
LB-1	79.7	17.8	2.5	4.5
LB-2	68.4	29.4	2.2	2.3
LB-3	77.5	20.1	2.4	3.8
LB-4	72.9	24.7	2.4	3.0

*The number of structural units of the p-coumaric (H) type was calculated by the formula 100-(G+S).

As already mentioned above, the ratio of syringyl, guaiacyl and p-coumaric structures is a very important characteristic of any lignins, since it can affect the number of active functional groups, as well as the features of the topological structure of macromolecules. Therefore, we estimated the number of these structures by various independent methods. The most tested and classical method is nitrobenzene oxidation and NMR-^{13}C [25]. The analysis with pyrolytic chromatography mass spectrometry is no less efficient and tested. The pyrolytic chromatogram for the LB-1 sample is shown in Figure and Table in the electronic supplement. Table 5 shows the results of determining the structural units by the above methods for one of the main studied samples LB-1. As the comparison of the data shows, all analytical methods give qualitatively identical results. This means that the conclusion based on the IR Fourier spectroscopy data that the lignin from the stem part contains the highest percentage of syringyl structures is quite justified.

Thus, it is shown that FTIR is a reliable method for evaluating the monomeric composition of lignin macromolecules.

EPR spectroscopy. As is known, all types of lignins have a unique property of paramagnetism. The presence of spins in lignins is conditioned by the structural features of macromolecules, the biosynthesis of which occurs by the mechanism of enzymatic free radical polymerization. At the final stage of biosynthesis, a high-molecular compound with paramagnetic properties is formed. These properties are conditioned by the presence of phenoxyl-type free radicals, the stability of which is determined by the length of the conjugation chain of double carbon-carbon bonds and the presence of benzene ring substituents [26]. Apparently, it is the presence of phenoxyl radicals that imparts the antioxidant function to lignins, which they perform in plants. In particular, LB-1 sample is characterized by AOA 78.6 kC/100 g, which exceeds AOA of Rutoside (Latin Rutosidum) equal to 61.0 kC/100 g [27, 28]. This vitamin is a recognized antioxidant drug, which is prescribed for the prevention of viral and infectious diseases, allergies and oncology. Thus, we have determined that lignins of woody plants, as well as lignins of herbaceous plants, have a high AOA, which opens up prospects for their biomedical applications. Of great interest is the comparison of the paramagnetic properties of lignins isolated from different vegetative organs of the forest stand. As the analysis shows (Fig. 3), the shape of the EPR signal of all the studied samples has some asymmetry, but is generally close to Lorentzian. The spectra are a singlet line, the width of which is determined by the spin density ΔB_{PP}. The shape of EPR signal is conditioned by the competing effects of narrowing and broadening of the spectral line. The first effect is associated with the delocalization of free electrons over the system of conjugated double bonds, the second – with the unresolved hyperfine structure of protons. In addition, the shape of the signal is affected by the distributed nature of the g-factors and the dipole interaction of spins [29].

Table 6 shows the values of the g-factors, ΔB_{PP} and the concentration of free radicals N. As follows from the obtained data, the lignin samples have similar values of g-factor, which is 2.0042±0.0001. The minimum line width ΔB_{PP} is set for the LB-2 sample, which is 0.50 mT. For the remaining samples, ΔB_{PP} values are almost the same and equal to 0.7 mT.

As is known, ΔB_{PP} characterizes the size of the free electron delocalization system. In this case, all the values of the spectral parameters correspond to the phenoxyl radicals of phenylpropane units, which are the main building blocks of all lignins. The lowest value of the concentration of carbon radicals N was found for the lignin sample isolated from burl, and the highest one was found in the sample from birch branches. It should be noted that the previously identified relationship between the number of spins N and the amount of phenolic hydroxyls (Table 3), as shown in [30], is not detected in this case. Therefore, it can be assumed that the paramagnetic properties of the samples will not play a significant role in the processes of thorium sorption-desorption. It is possible that a more important influence on them can be exerted by the features of the topological structure of macromolecules.

Table 5. The content (%) of S, G and H units (%) for LB-1 sample according to the different methods of NMR-^{13}C, Py-GC/MS, NBO and FTIR-spectroscopy

Method	S	G	H
FTIR	79.7	17.8	2.5
Py-GC/MS	74.6	25.4	0
NBO*	77.3	22.7	0
NMR-^{13}C*	74.6	24.6	0.8

* The results are presented in [25]

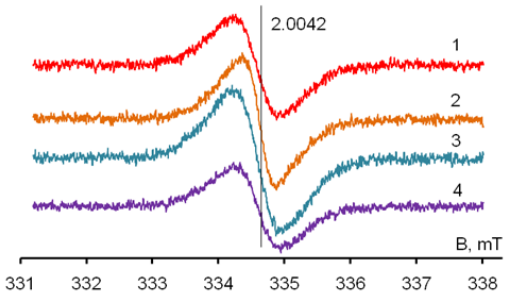


Fig. 3. EPR spectra of samples of lignin LB-1 (1), LB-2 (2), LB-3 (3) and LB-4 (4)

*Macromolecular properties and topological structure***.** Polymer-based adsorption materials have a very complex structural organization of a hierarchical type. For high-molecular compounds, in order of increasing scale level, molecular (chemical), macromolecular (topological) and supramolecular levels are distinguished. Previously [31–33] an assumption was made about the possible influence of the topological structure of macromolecules on the adsorption characteristics of lignins. In this case, the assessment of the degree of influence was based on the determination of the compactness and density of macromolecular balls, which in turn depended on the topology of the macromolecule. We conducted studies of the macromolecular structure of the samples under study, as well as additionally lignin isolated from the trunk of the dwarf birch *Betula nana* (LB-1n). Table 7 presents the experimental hydrodynamic characteristics of the macromolecules obtained using a set of classical methods: velocity sedimentation, translational diffusion and capillary viscometry. This allowed establishing the topology of the lignin samples under study (Table 7).

According to the obtained results, the highest molecular weight polymer is sample LB-1 with *Mw* value of 14.7×10^3 Da. The lignin sample LB-3, isolated from the branches, turned out to be the lowest molecular weight polymer, with an average molecular weight of 6.6×10^3 Da. To identify the type of topology of the lignin samples, a detailed analysis of the key structural indicators characterizing the topological level of the structural organization of the polymers was carried out. Table 6 shows values of the hydrodynamic Flory-Mandelkern (FM) invariant, the Tsvetkov-Klenin (A0) invariant, the Mark-Kuhn-Houwink-Sakurada (MKHS) scaling indices b_i and the fractal dimension of self-similarity d_F. First of all, attention should be paid to the values of the hydrodynamic Tsvetkov-Klenin invariant A_0, which differ significantly from the typical values for linear polymers. For natural and synthetic flexible-chain polymers, A_0 is $(3.2\pm0.2)\times10^{-10}$ erg×K^{-1}mol$^{-1/3}$, or even slightly higher (for rigid-chain polymers) [37, 38]. For branched polymers, including star-shaped ones with linear branches, this figure is significantly lower and can reach ~2.0×10^{-10} erg×K^{-1}mol$^{-1/3}$ [39, 40]. As theory and practice show, the Flory-Mandelkern invariant value for linear macromolecules is 2.3×10^{-6}. For the samples under study, this parameter does not exceed 2.0×10^{-6} (Table 7). Thus, as follows from the analysis of the hydrodynamic invariants, all the lignins under study clearly belong to the category of branched polymers. Among the most probable configurations, we can distinguish the chaotically branched, star-shaped and network types. To identify the type of polymer branching, the MKHS scaling indices b_η and b_D (Table 7) are important, characterizing the behavior of macromolecules under rotational and translational friction. These indicators are established, as is known, in independent experiments to assess the intrinsic viscosity [η] and translational diffusion D, which increases the reliability of the conclusions obtained. Figure 4 presents the results of the evaluation of the relationship between the intrinsic viscosity [η] and the translational diffusion coefficients D for the fractionated preparations LB-1 and LB-3, which indicate the feasibility of the scaling principle. In addition, they confirm the topological homogeneity of the studied lignins, which allows us to obtain correct data on the scaling indices of the MKHS.

Table 6. Parameters of the organic radical line of lignin samples

Sample	ΔB, mT	g	N, 10^{17} spin/g
LB-1	0.69	2.0043	0.8
LB-2	0.50	2.0041	0.8
LB-3	0.73	2.0042	1.2
LB-4	0.72	2.0042	0.7

Table 7. Macromolecular characteristics of lignin samples and model fractal clusters of various types

Sample	$M_w \times 10^{-3}$, Da	CPS	b_η	$\lvert b_D \rvert$	d_f*	FM×10^{-6}	$A_0 \times 10^{10}$ эрг K^{-1} моль$^{-1/3}$	Topological structure
LB-1	14.7	1.22	0.57±0.03	-0.55±0.05	1.91/1.8	1.59	2.2	Star-like
LB-1n	7.6	–	0.65±0.02	-0.54±0.03	1.86/1.7	1.88	2.6	Star-like
LB-2	11.3	1.6	0.27±0.02	0.33	2.36/2.4	1.59	2.19	Chaotically branched
LB-3	6.6	1.8	0.29±0.01	0.34±0.10	2.32/2.4	1.86	2.57	Chaotically branched
LB-4	14.0	0.6	0.31±0.04	0.43±0.04	2.29/2.2	2.0	2.83	Chaotically branched
DLA Cl-Cl [34]	–	–	0.5–0.7		1.75–2.0		–	Star-like
DLA P-Cl [35, 36]	–	–	0.2–0.5		2.0–2.5		–	Chaotically branched

* In the numerator, of the viscosimetric scaling index; in the denominator, by the Kozlov-Temirayev- Sozaev equation.

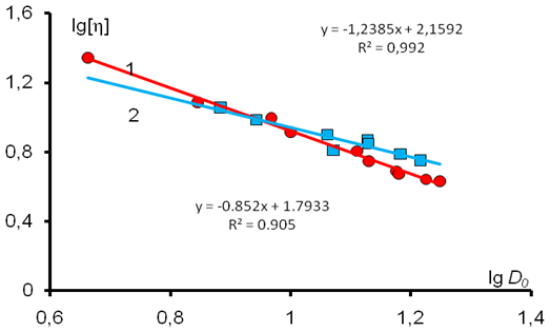


Fig. 4. Dependency lg[η] – lg D_0 for samples LB-1 (1) and LB-3 (2)

Data analysis shows that samples LB-1 and LB-1n, on the one hand, and samples LB-2, LB-3 and LB-4, on the other hand, have fundamentally different conformational and scaling characteristics. One of the most sensitive parameters characterizing the structure of the macromolecular coil is the viscosimetric index of the MKHS b_η. As is known [34, 39], the value of this indicator for linear polymers fluctuates in the range of 0.5-07. For branched polymers, this indicator usually varies in the range of 0.2–0.4. As can be seen from the obtained data, for samples LB-2, LB-3 and LB-4, the b_η value falls within this range, with $b\eta < \lvert b_D \rvert$, which clearly indicates the branching of the macromolecules of these samples.

For samples LB-1 and LB-1n, the opposite picture is observed: $b\eta > \lvert b_D \rvert$. And this corresponds to polymers with a linear topology. Thus, the hydrodynamic behavior of LB-1 and LB-1n macromolecules demonstrates duality: some indicators correspond to linear polymers, and others - to branched structures. Analysis of the entire set of experimental data allows us to conclude that LB-1 and LB-1n macromolecules belong to the class of regularly branched polymers with linear chains, that is, to the class of star-shaped macromolecules. Our computer modeling of the growth of linear, star-shaped and chaotically branched macromolecular structures and the assessment of their scaling indices and fractal dimension (Table 6) are consistent with these findings. Can the topology of macromolecules affect the processes of sorption-desorption of the thorium radionuclide? In our opinion, such an influence is possible, but not directly, but indirectly. In essence, in this case it is necessary to link the topology with the density (compactness) of the macromolecular coil. The density of the coil is predetermined by the type of macromolecule topology and the value of the fractal dimension, which serves as a measure of the occupancy of the embedding space of the object. Hydrodynamic measurements allowed us to determine the fractal dimension of self-similarity d_f of macromolecules (Table 6). According to classical concepts, a linear macromolecule forms a looser coil ($1.7<d_f<2$)than a branched one ($d_f>2$). Thus, the higher the value of the fractal dimension, the higher the density the macromolecular coil. For example, the fractal dimension of the network polymer is 3.0. The fractal dimension of LB-2, LB-3 and LB-4 is quite high: 2.2–2.4, which is consistent with their classification as chaotically branched

polymers. Modeling the growth of macromolecules by the mechanism of diffusion-limited aggregation of the particle-cluster type (DLA P-Cl) shows that chaotically branched lignins are fractal clusters of the Witten-Sander type, characterized by increased compactness and density. Significantly looser cluster structures of the linear and star-shaped type are formed within the framework of the model of diffusion-limited aggregation of the cluster-cluster type (DLA Cl-Cl). Thus, the obtained results show that the studied samples of birch lignins differ from each other in the density of macromolecular balls, which is characterized in terms of the fractal concept. Comparison of the values of the adsorption indices A_F in relation to the radionuclide thorium-232 and the fractal dimension indicates the existence of a certain relationship. This relationship is described by the equation: $A_F = 263.0 - 89.3d_f$ with the correlation coefficient R = -0.737. In our opinion, the phenomenon of the influence of the topological structure on the adsorption processes is explained by the effect of screening a certain part of the active functional groups of the polymer when folding macromolecules into a ball, since a star-shaped macromolecule is a less dense structure than a chaotically branched one.

Conclusion

The results of the study of the chemical structure, spectral, paramagnetic and adsorption properties of lignins isolated from various vegetative parts of a birch stand are presented. It has been established that Birch lignins have a unique ability to chemical and topological diversity. It is shown that IR spectroscopy is a reliable method for determining the structural elements of G, S and H types. It has been established that the ionogenic functional groups, carboxylic and phenolic, play an important role in the adsorption process. The lignin from the stem has a star-shaped topology, while lignins from branches, roots and a growth on the trunk are chaotically branched polymers. It is suggested that the topology of macromolecules may influence the sorption capacity of lignins. The obtained results expand the database of the biomedical properties of lignins, which can be used to develop innovative biologically active enterosorbents of the next generation.

Supplementary Information
The electronic supplement to the article (DOI: http://www.doi.org/10.14258/jcprm.20260418421s) provides additionalexperimental material that reveals the main points set out in the article.

Acknowledgements
This work was performed using the instrumentation of the Core Facility Center "Molecular Biology" of the Institute of Biology of the Komi Science Center UB RAS.

Funding
The study was carried out at the expense of a grant from the Russian Science Foundation № 22-13-00196-P, https://rscf.ru/en/project/22-13-00196/.

Conflict of Interest
The authors of this work declare that they have no conflicts of interest.

Open Access
This article is distributed under the terms of the Creative Commons Attribution 4.0 International License (https://creativecommons.org/licenses/by/4.0/), which permits unrestricted use, distribution, and distribution in any medium provided you give appropriate credit to the original author(s) and the source and link to the Creative Commons license, and indicate if they were modified.

References

1. Fesenko S., Emlutina E. *Biology Bulletin*, 2021, vol. 48, pp. 2086–2097. https://doi.org/10.1134/S1062359021110030.
2. Kolesnik O., Rozhko T., Kudryasheva N. *International journal of molecular sciences*, 2022, vol. 24, pp. 410–428. https://doi.org/10.3390/ijms24010410.
3. Anderson C., Johnsson A., Moll H., Pedersen K. *Geomicrobiology Journal*, 2011, vol. 28, pp. 540–561.
4. Hu Q., Weng J., Wang J. *Journal of environmental radioactivity*, 2010, vol. 101, pp. 426–437. https://doi.org/10.1016/j.jenvrad.2008.08.004.
5. Brugge D., deLemos J., Oldmixon B. *Reviews on Environmental Health*, 2005, vol. 20, pp. 177–189. https://doi.org/10.1515/REVEH.2005.20.3.177.
6. Fatullayeva S., Tagiyev D., Zeynalov N. *Colloid and Interface Science Communications*, 2021, vol. 45, 100545. https://doi.org/10.1016/j.colcom.2021.100545.
7. Fatullayeva S., Tagiyev D., Zeynalov N., Raucci M., Amendola E., d'Ayala G., Suleymanova R. *Carbohydrate Research*, 2024, vol. 545, 109255. https://doi.org/10.1016/j.carres.2024.109255.
8. Mikhalovsky S., Voytko A., Demchenko V., Demchenko P. *Chemistry journal of Moldova*, 2021, vol. 16, pp. 9–27. https://doi.org/10.19261/cjm.2021.852.

9. Gupta D., Voronina A., Semenishchev V., Chatterjee S. *Green Adsorbents for Pollutant Removal. Innovative materials*, 2018, pp. 377–396.
10. Wang B., Sun Y., Sun R. *Journal of Leather Science and Engineering*, 2019, vol. 1, pp. 1–25. https://doi.org/10.1186/s42825-019-0003-y.
11. Chopabayeva N. *Journal of Composites and Biodegradable Polymers*, 2017, vol. 5, pp. 1–9. https://doi.org/10.12974/2311-8717.2017.05.01.1.
12. Ali A., Mehanna M. *Int. J. Biol. Macromol*., 2022, vol. 221, pp. 934–953. https://doi.org/10.1016/j.ijbiomac.2022.09.007.
13. Shu F., Jiang B., Yuan Y., Li M., Wu W., Jin Y., Xiao H. *Biomacromolecules*, 2021, vol. 22, pp. 4905–4918. https://doi.org/10.1021/acs.biomac.1c00805.
14. Tobimatsu Y., Schuetz M. *Current opinion in biotechnology*, 2019, vol. 56, pp. 75–81. https://doi.org/10.1016/j.copbio.2018.10.001.
15. Ralph J., Lapierre C., Boerjan W. *Current opinion in biotechnology*, 2019, vol. 56, pp. 240–249. https://doi.org/10.1016/j.copbio.2019.02.019.
16. Pepper J., Baylis P., Adler E. *Can. J. Chem*., 1959, vol. 37, pp. 1241–1245.
17. Zakis G. *Funktsional'nyy analiz ligninov i ikh proizvodnykh* [Functional Analysis of Lignins and Their Derivatives]. Riga, 1987. 230 p. (in Russ.).
18. Singh N., Nagpal G., Agrawal S. *Environmental technology & innovation*, 2018, vol. 11, pp. 187–240. https://doi.org/10.1016/j.eti.2018.05.006.
19. Thommes M., Kaneko K., Neimark A., Olivier J., Rodriguez-Reinoso F., Rouquerol J., Sing K. *Pure and Applied Chemistry*, 2015, vol. 87, pp. 1051–1069. https://doi.org/10.1515/pac-2014-1117.
20. Karmanov A., Kocheva L., Belyy V., Kanarsky A., Semenov E., Bogdanovich N., Pokryshkin S. *Biocatalysis and Agricultural Biotechnology*, 2023, vol. 54, 102969. https://doi.org/10.1016/j.bcab.2023.102969.
21. Dokken K., Davis L., Marinkovic N. *Applied Spectroscopy Reviews*, 2005, vol. 40, pp. 301–326
22. Karmanov A., Derkacheva O., Kocheva L., Kanarsky A., Semenov E., Demin V., Bogdanovich N. *J. Sib. Fed. Univ. Chem*., 2023, vol. 16, pp. 595–607.
23. Popukailo V. *Technology and design in electronic equipment*, 2016, vol. 4-5, pp. 42–46.
24. De Winter J. *Practical assessment, research & evaluation*, 2013, vol. 18, 10. https://doi.org/10.7275/e4r6-dj05.
25. Evstigneev E.I. *Russian Journal of Bioorganic Chemistry*, 2025, vol. 51, no. 7, pp. 2881–2903.
26. Su X., Fu Y., Shao Z., Qin M., Li X., Zhang F. *Ind. Crop. Prod*., 2022, vol. 176, 114359. https://doi.org/10.1016/j.indcrop.2021.114359.
27. Borisenkov M., Karmanov A., Kocheva L. *Adv. Gerontol*., 2005, vol. 17, pp. 34–41.
28. Kocheva L., Borisenkov M., Karmanov A., Mishurov V., Spirikhin L., Monakov Y. *Russian journal of applied chemistry*, 2005, vol. 78, pp. 1343–1350. https://doi.org/10.1007/s11167-005-0512-8.
29. Gourier D., Binet L., Scrzypczak A., Derenne S., Robert F. *Spectrochimica Acta Part A. Molecular and Biomolecular Spectroscopy*, 2004, vol. 60, pp. 1349–1357. https://doi.org/10.1016/j.saa.2003.10.033.
30. Karmanov A., Shaposhnikova L., Kocheva L., Rachkova N., Belyi V., Lutoev V., Tumaeva P. *Chemistry & Biodiversity*, 2025, e202500624. https://doi.org/10.1002/cbdv.202500624.
31. Duval A., Lawoko M. *Reactive and Functional Polymers*, 2014, vol. 85, pp. 78–96. https://doi.org/10.1016/j.reactfunctpolym.2014.09.017.
32. Karmanov A., Kanarsky A., Kocheva L., Belyy V., Semenov E., Rachkova N., Bogdanovich N., Pokryshkin S. *Polymer*, 2021, vol. 220, 123571. https://doi.org/10.1016/j.polymer.2021.123571.
33. Kozhevnikov A.Y., Shestakov S.L., Sypalova Y.A. *Khimiya rastitel'nogo syr'ya*, 2023, no. 2, pp. 5–26. https://doi.org/10.14258/jcprm.20230211737. (in Russ.).
34. Meakin P. *J. Sol-Gel Sci. Technol*., 1999, vol. 15, pp. 97–117. https://doi.org/10.1023/A:1008731904082.
35. Witten T., Sander L. *Phys. Rev. Lett*., 1981, vol. 47, pp. 1400–1403.
36. Karmanov A. *Samoorganizatsiya i strukturnaya organizatsiya lignina* [Self-organization and structural organization of lignin]. Ekaterinburg, 2004, 270 p. (in Russ.).
37. Tsvetkov V., Eskin V., Frenkel S. *Structure of Macromolecules in Solution*. London, 1970.
38. Tsvetkov V., Lavrenko P., Bushin S. *J. Polym. Sci*., 1984, vol. 22, pp. 3447–3486
39. Pavlov G., Knop K., Okatova O., Schubert U. *Macromolecules*, 2013, vol. 46, pp. 8671–8679. https://doi.org/10.1021/ma400160f.
40. Shpyrkov A., Tarasenko I., Pankova G., Il'ina I., Tarasova E., Tarabukina E., Vlasov G., Filippov A. *Polym Sci*., 2009, vol. 51, pp. 250–258. https://doi.org/10.1134/S0965545X09030031.

Received December 17, 2025

Revised June 23, 2026

Accepted November 17, 2026

Information about authors

Karmanov Anatoly Petrovich – Leading Research Scientist, e-mail: apk0948@yandex.ru

Kocheva Lyudmila Sergeevna – Leading Research Scientist, e-mail: karko07@mail.ru

Rachkova Natalya Gelievna – Head of the Laboratory, e-mail: rachkova@ib.komisc.ru

Derkacheva Olga Yurievna – Senior Research Fellow, e-mail: derkachevaou@rambler.ru